International Journal of Medical Physics, Clinical Engineering and Radiation Oncology, 2026, 15(2), 29-40
https://www.scirp.org/journal/ijmpcero
ISSN Online: 2168-5444
ISSN Print: 2168-5436

Characterizing the Variations of Dose Delivery to Coronary Vessels for Sr-90/Y-90 IVBT Using Monte Carlo Simulations

Nicholas Coupera[1,2], Yijan Cao[1,2,3,4], Jenghwa Chang[1,2,3,4*]

[1]Northwell, New Hyde Park, USA
[2]Department of Radiation Medicine, Northwell Health, Lake Success, USA
[3]Zucker School of Medicine at Hofstra/Northwell, Hempstead, USA
[4]Department of Physics and Astronomy, Hofstra University, Hempstead, USA
Email: *jchang24@northwell.edu

How to cite this paper: Coupera, N., Cao, Y. and Chang, J. (2026) Characterizing the Variations of Dose Delivery to Coronary Vessels for Sr-90/Y-90 IVBT Using Monte Carlo Simulations. *International Journal of Medical Physics, Clinical Engineering and Radiation Oncology*, **15**, 29-40.
https://doi.org/10.4236/ijmpcero.2026.152003

Received: February 2, 2026
Accepted: April 17, 2026
Published: April 20, 2026

Abstract

Purpose: To quantify using Monte Carlo simulations the variations of dose delivery to coronary vessels undergoing treatment by Sr-90/Y-90 intravascular brachytherapy (IVBT). **Material and Methods:** The Novoste Beta-Cath 3.5 F Sr-90/Y-90 pure beta-emitting source and geometry were modeled in GATE, open-source Monte Carlo software based on the Geant4 toolkit. Source spectrum through the stainless-steel capsule and flexible jacket were verified by comparing the simulated percent depth dose curve with the manufacturer's data sheet. Dose distribution to the nominal vessel geometry (3.2 mm in diameter, 1.1 mm wall thickness, no stent) were calculated, and the variations of dose delivery were characterized as the dose ratio with and without perturbations due to implanted metallic stents, calcified plaques, variable vessel diameter, and sources offset from center. **Results:** A dose reduction of up to 26% was found throughout the vessel due to the presence of a stent, dependent on stent material, metallic surface area, and strut thickness. The introduction of calcified plaque further reduced vessel doses by up to 40%. The doses given to the smallest vessels in their prescription category were 34% higher than those to the largest vessels. Random motion of the source from excess space inside the 3.5 F catheter leads to an up to 18% increase in dose depending on the size of the vessel. **Conclusion:** The dose effects from these often-unavoidable perturbations in the nominal vessel geometry are found to be significant and attempts should be made to account for these effects in accurate dose calculations. The authors recommend a refining of the current prescriptions based on vessel diameter, so the largest and smallest vessels have <20% dose variation.

Keywords

IVBT, Monte Carlo Simulation, Dosimetry

1. Introduction

Intravascular brachytherapy (IVBT) is a procedure *in which radioactive sources are temporarily delivered* via catheter to a coronary artery following balloon angioplasty. During the angioplasty procedure, an ischemic coronary artery is first expanded by balloon catheter, and a stent, either bare metal or drug-eluting, is inserted to hold the artery open. Bare metal stents can lead to restenosis *due to excessive* proliferation of the neointima which results in adventitial fibrosis. Drug-eluting stents can also result in restenosis, which is thought to result from hypersensitivity to polymer and drug, local inflammation, mechanical factors, and delayed healing leading to neointimal proliferation [1]. The goal of IVBT is therefore to prevent restenosis by locally damaging the neointima with radiation. IVBT provides an advantage in its high localization of dose, minimizing toxicities to normal tissues such as the heart. With 500,000 balloon angioplasty procedures performed per year in the US [2] and 5% - 6% of drug-eluting stents leading to restenosis [3], there is *significant potential benefit in* treating with IVBT and studying its dosimetric qualities.

The Beta-Cath system, developed by the Novoste Corporation, is the first approved β-particle IVBT device. As shown in **Figure 1**, this hand-held delivery device stores a "train" of Sr-90/Y-90 sources. Sr-90 and Y-90 exist in secular equilibrium with average β energies of 196 keV and 934 keV, respectively [4]. The train is hydraulically advanced and retracted with sterile saline solution. Each source is 2.5 mm long, and the trains are available in 30, 40, and 60 mm lengths for various lengths of lesions. The train travels through a 3.5 F (1.16 mm) catheter which is guided through the same guide catheter used in the preceding angioplasty. It should be noted that the guide wire used to navigate to the coronary artery is removed prior to irradiation and does not perturb the dose delivery. Dose is prescribed nominally to a point 2 mm from the center of the source, with

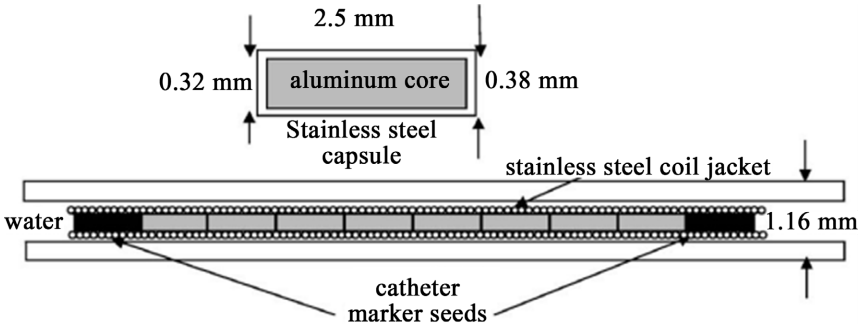

Figure 1. Schematic showing 3.5 F single seed of Sr-90/Y-90 and an 8-seed train with Pt/Ir markers at the ends in a stainless-steel wire jacket.

calibrations performed in water [5]. Vessels between 2.7 - 3.3 mm in diameter are prescribed a dose of 18.4 Gy, while vessels between 3.4 - 4.0 mm in diameter are prescribed a dose of 23.0 Gy. These doses were calculated by the National Institute of Standards and Technology (NIST) based on the Stents and Radiation Therapy (START) trials [6].

In this study, Monte Carlo simulations of Sr-90/Y-90 IVBT treatments are run with varying scenarios, representing possible variations of real treatments, to observe their dosimetric effects. Dosimetry at distances on the order of millimeters, especially for β-sources, are difficult to calculate and measure. Monte Carlo simulation provides the most accurate way to calculate doses in these cases and are simple to repeat or modify after initial setup. The simulations comprised varying vessel diameter, simulating vessel movement during treatment, varying coronary stent material and metal surface area (MSA), and varying calcified plaque thickness. Each of these scenarios may be present to different degrees in IVBT treatments and providers should be aware of them when prescribing.

2. Material and Methods

Monte Carlo simulations for this study were performed with GATE, a GEANT4-based Monte Carlo simulation tool developed by the OpenGATE Collaboration [7]. GATE is useful in its ability to simulate custom source decays, materials, and geometries, and utilizes the well-validated physics models of GEANT4. The package was installed on an independent workstation with an Ubuntu 22.04.5 operating system. The physics processes simulated included Compton, photoelectric, and pair production for photons; electron ionization, continuous slowing down approximation (CSDA) model, and bremsstrahlung for electrons and positrons. The PENELOPE (Penetration and Energy Loss of Positrons and Electrons) models of GEANT4 were chosen for the electromagnetic processes. This particular installation of GATE including all physics processes modeled has been validated for accuracy in a previous study by Chang *et al.* [8].

The "nominal geometry" which served as the basis for simulations included the Sr-90/Y-90 source train, its stainless-steel jacket, the coronary vessel, blood inside the vessel, and water outside the vessel. The source train was 40 mm long, comprised of 16 cylindrical sources 0.32 mm diameter and 2.44 mm long, surrounded by a stainless-steel capsule uniformly 0.03 mm thick. The sources have aluminum composite cores and so aluminum was chosen as the material in the simulation. The stainless-steel jacket, in reality a coil of wire, was modeled as a hollow cylinder of inner diameter 0.42 mm and outer diameter 0.47 mm. This was due to limitations of creating such a geometry in the program. **Figure 2** illustrates a simulation visualization of Sr-90/Y-90 source in the nominal vessel geometry. The vessel wall, approximated with a muscle material, had a 3.2 mm inner diameter and 4.3 mm outer diameter. The space between the source and the vessel was filled with blood. To measure the average dose to the vessel wall, *hereafter referred to as* wall dose, a rectangular detector was placed with its center at the center of one side of the

vessel wall. The width was the thickness of the wall, and the height was 0.4 mm. The length was 30 mm, spanning the middle three quarters of the total source train length. Dose was calculated by GATE by summing each history that deposited energy into the detector volume and dividing by the mass of the vessel material in the volume. Per history dose was calibrated by normalizing to the 2 mm nominal prescription point. Each simulation tracked approximately 10^7 histories, which was enough to bring dose uncertainties to around 1% or less.

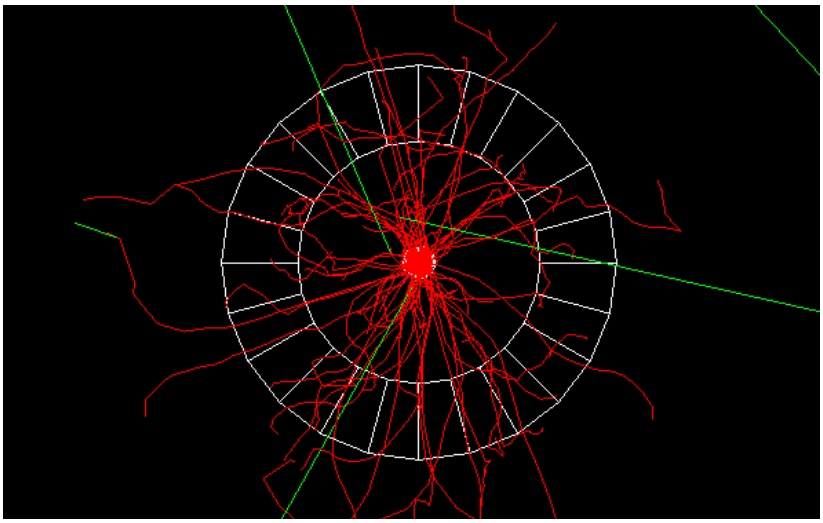

Figure 2. Simulation visualization of Sr-90/Y-90 source in the nominal vessel geometry. Electron tracks are shown in red and photon tracks are shown in green.

The thickness of the steel jacket surrounding the source train was chosen by comparing the simulated percent depth dose (PDD) to the manufacturer's supplied PDD. Simulated PDDs were calculated for the central one third of the source train, in water, including the steel jacket and catheters. The Pt/Ir markers were not included in the simulation due to their distances (>1.6 cm) from the points of measurement. Since the actual jacket is a coil, and GATE does not provide for such geometries, an effective thickness needed to be found for its approximation as a hollow cylinder. Different thicknesses of the jacket were simulated, and the sum of square differences of the PDDs was optimized for, from 0.75 mm to 6.5 mm from the center of the sources. A 0.4 mm thick rectangular detector recorded the PDD at 0.25 mm resolution perpendicular to the source. The lowest sum of square differences was 0.0756 using a wall thickness of 0.025 mm. The average of the absolute value of percent differences was 2.87%, with the largest single percent difference being 6.9%. This served to validate that the modeled source was very close to the actual one.

To measure the effect of vessel diameter on wall dose, the nominal geometry was used and only the vessel wall inner and outer diameters were adjusted to maintain a constant vessel wall thickness. The simulation was run with vessel wall inner diameter from 2.7 mm to 3.3 mm in 0.2 mm increments, and again from 3.4 mm to 4 mm with the same increment. These two ranges represent the ranges of

allowed vessel size for the 18.4 Gy and 23 Gy nominal prescriptions, respectively. Since these are nominal prescriptions, representing the dose to 2 mm from the center of the source, the wall dose naturally decreased as the diameter increased. Though vessels outside of the prescribed diameter ranges might still be treated, they were not considered in this study.

The Beta-Cath delivery system has no means of centering the source within the guide catheter, nor the guide catheter within the vessel. Motion can therefore take place which brings the source closer or farther from the vessel wall, within the geometrical constraints of the catheters and vessel diameter. This is illustrated in Figure 3 which shows the largest radial distance of the source allowed by the geometries. In this study, the effect of motion of coronary arteries, such as from the heart beating, was simulated by moving the center of the source relative to the center of the vessel wall. The source was moved to 500 random locations over each simulation to simulate totally random motion over a treatment time that is long compared to the frequency of motion. Any position within the vessel was allowed so long as the source, jacket, and 2 catheters were not intersecting with the vessel wall. The radius and angle of deviation from the center of the vessel were chosen from a uniform distribution over their range. The guide catheter and 3.5 F catheters have wall thicknesses of 0.1 mm and 0.215 mm, respectively. This meant the source was free to move within a radius of (r-0.55 mm), after accounting for the thickness of the source and jacket, where r is the inner radius of the vessel wall.

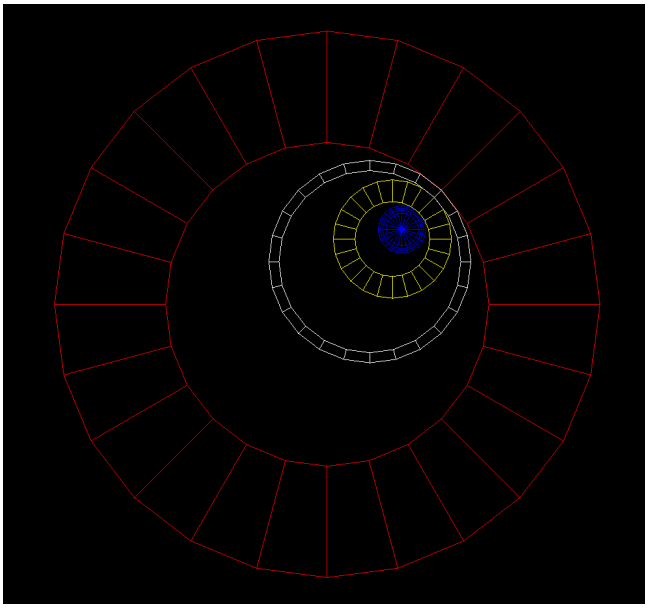

Figure 3. Geometry visualization of the source (blue), catheters (yellow), guide catheter (white), and vessel (red), when random motion is included. This shows the largest radial distance of the source allowed by the geometries.

To evaluate the dose effect of stents, the stent geometries first had to be simplified. Stents come in a variety of shapes, thicknesses, and surface areas, and summarizing the differences from all three would be cumbersome and impractical.

Instead, the shapes of the stents were simplified to stacked rings, where each ring was 0.1 mm in height and separated by a gap determined by the metal surface area (MSA). The rings had the same outer diameters as the inner diameters of the vessel wall, since they hold the vessel open. The shape is assumed to have little overall effect on the wall dose, and this shape was the easiest to implement in the simulation. A series of simulations were then run by varying the stent thickness for a fixed MSA, and the result was found to be linear, with an R^2 of 0.9841. This allowed the comparisons to focus on MSA, where stent thicknesses of 0.1 mm were used exclusively. Dose effects from a different thickness of stent would simply be proportional to the thickness. Finally, dose effects were measured for 3 different stent materials, nitinol, tantalum, and stainless steel, in only one variable, MSA.

Lastly, to measure the dose effect of calcified plaques in the arteries, a hollow cylinder of plaque material was added just inside the vessel wall. The density and calcium content of plaques as reported in Rahdert *et al.* [9] and Moselewski *et al.* [10], respectively, were used in the simulation. The inner diameter of the plaque would be the same as the nominal vessel diameter, with the vessel wall expanded to include the whole plaque. This was done because a balloon expansion of the vessel was assumed, wherein the plaque would remain inside the vessel and force the vessel to expand around it. This led to there being two dosimetric effects from the plaque. First the absorption of the β-rays by the plaque before reaching the vessel wall, and second the widening of the vessel wall itself. These effects were separated from the total effect by comparing the simulations to ones with the same expanded vessel wall, but no plaque.

3. Results

Figure 4 plots simulated average dose to 1.1 mm thick vessel wall vs vessel inner diameter. As shown in **Figure 4**, wall dose decreases within each *prescription group as* vessel diameter increases, consistent with expectations. There is a large variation in delivered doses by diameter, even within the prescription ranges. A vessel of 3.3 mm diameter receives 29.7% less dose than a 2.7 mm diameter vessel for the same 18.4 Gy nominal prescription. Within the 23 Gy prescription, a 4.0 mm diameter vessel receives 30.8% less dose than one 3.4 mm diameter. The 4.0 mm and 2.7 mm diameters also receive doses outside the range of doses found in the other prescription. This demonstrates the inconsistency of the current prescriptions in the extreme vessel size range. A possible solution would be to add a third prescription, so that each is used for a small range of vessel diameters.

Figure 5 shows the effect of random motion (such as from heartbeat) on the delivered wall dose. All vessel diameters see a dose increase from this motion, and a trend is observed for larger vessels to have a higher dose effect. This can be explained by the dose fall off for a line source. In the limit where the distance from the point of interest to the source is much less than the length of the line source, the dose falls off by a 1/r distribution. The percent increase in the dose from the source being in a closer position will therefore be greater than the percent decrease

from the source being the same amount farther away. Since the source spends the same amount of time, on average, on each side of the centerline, the average effect will result in a dose increase. The trendline indicates an approximate 7.9% increase in dose per 1 mm increase in vessel diameter.

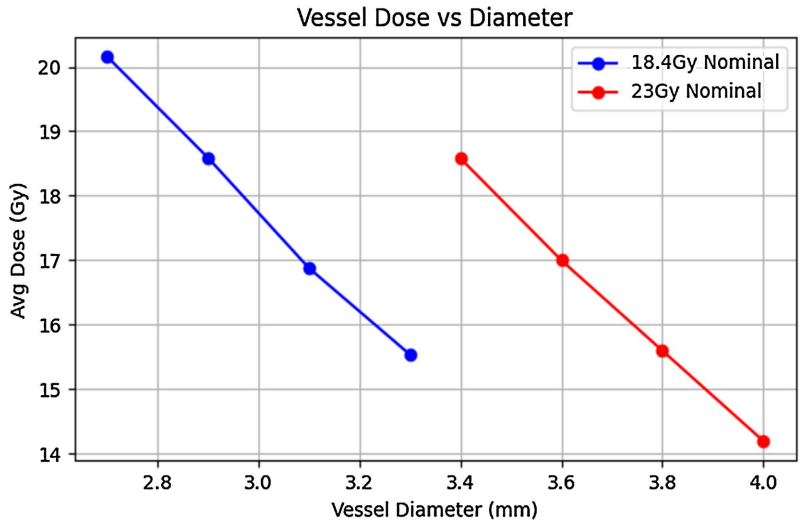

Figure 4. Plot of simulated average dose to 1.1 mm thick vessel wall vs vessel inner diameter.

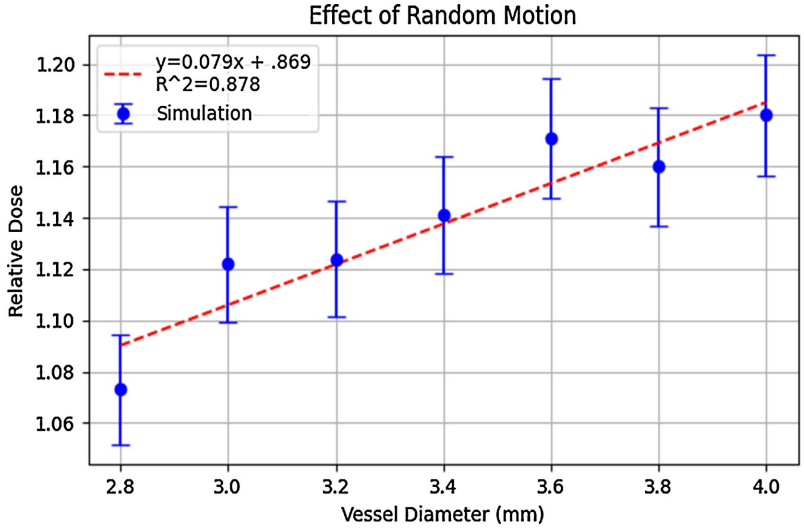

Figure 5. Plot of simulated average dose to 1.1 mm thick vessel wall vs vessel inner diameter when random source motion is introduced in the simulation. Doses are relative to simulations with no source motion.

Dose effects created in the presence of tantalum, nitinol, and stainless-steel stents are shown in **Figure 6**. Tantalum, with its high atomic number, showed the greatest decrease in dose, as expected. The effect was approximately 7% decrease in dose for a 10% increase in MSA. As nitinol and stainless steel have similar atomic numbers, their effects were understandably similar to each other. Both resulted in an approximately 3% decrease in dose per 10% increase in MSA. As mentioned, these results are for stents with a 0.1 mm thickness. To calculate the effect

from a stent of different thickness, the percent decrease in dose would be scaled linearly with the thickness, *i.e.* a 0.2 mm stent decreases the dose by twice as much.

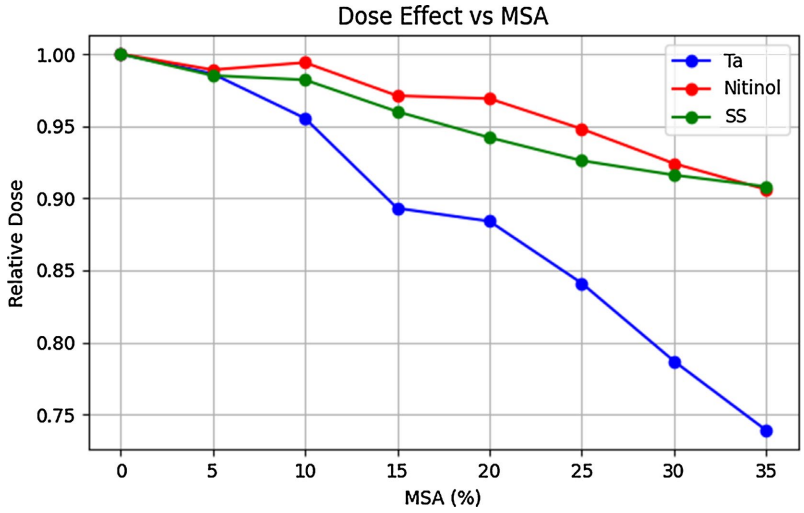

Figure 6. Plot of simulated average dose to 1.1 mm thick vessel wall vs stent metal surface area for tantalum, nitinol, and stainless steel stents.

Dose effects of plaque inside the vessel are shown in **Figure 7**. The calcified plaque, having a density and average atomic number higher than the surrounding vessel, contributes significantly to the absorption of the β-spectrum. However, the presence of plaque reduces the vessel dose much more simply by forcing the vessel to expand larger in the ballon angioplasty. This is labelled the diameter effect. One can treat the expansion and absorption effects as separate effects which are multiplied together. The combined effect reduces the vessel dose by approximately 8% per 0.1 mm of plaque. Removing the effect of the increased diameter, the plaque alone reduces the dose by approximately 2% per 0.1 mm.

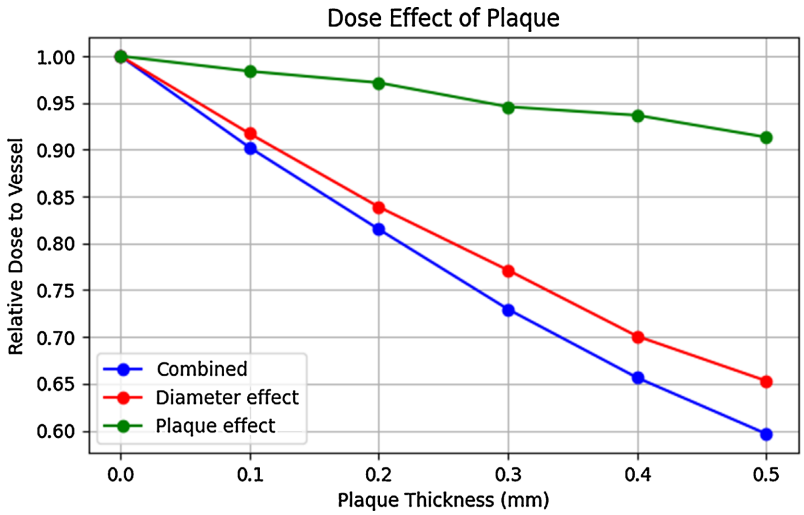

Figure 7. Plot of simulated average dose to 1.1 mm thick vessel wall vs thickness of plaque inside the vessel. Total dose effect is separated into absorption by plaque and increased diameter effects.

4. Discussion

In this study, a Sr-90/Y-90 IVBT β-source train was modeled, along with relevant treatment geometries, in Monte Carlo simulations. The accuracy of the simulation was previously validated, and further validations came from comparisons to the manufacturer's stated PDD. After verification, *simulations were performed incorporating variations from the "nominal geometry" that may occur in clinical treatments* to determine the dosimetric effects of those variations. Every variation was found to *produce substantial* (>10%) absolute dose effects on the wall dose delivered to the target vessel. It is therefore suggested that providers account for these effects to the best of their ability.

From Figure 4, it is apparent that much of the dose variation in treatments across vessel diameters comes from using only two prescription levels, small (2.7 - 3.3 mm) and large (3.4 - 4.0 mm). A vessel 4 mm in diameter treated to the nominal dose of 23 Gy receives 42% less average dose than a 2.7 mm vessel treated to 18.4 Gy nominal, representing the extremes of vessel diameters for IVBT. A *straightforward approach to reducing this variation would be to introduce* a third prescription level, as shown in Figure 8. This example leads to a dose variation of no more than 20% across the range of treatable diameters. The specific dose levels were chosen to coincide with the maximum and minimum doses delivered to large and small vessels, respectively. Another solution would be to compute the nominal dose uniquely for each vessel diameter. This could theoretically give equal average dose to every vessel, regardless of size. Justification of what the nominal dose(s) should be would necessarily rely on retrospective studies of patient outcomes, which are not included in this work.

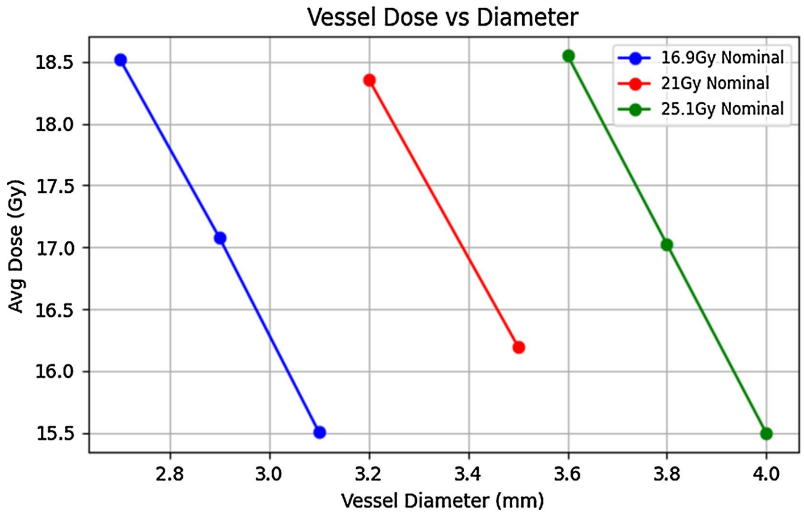

Figure 8. Plot of simulated average dose to 1.1 mm thick vessel wall vs vessel inner diameter for an example prescription where 3 dose levels are used. Dose levels are chosen to keep near equal average vessel dose across all diameters.

The random motion of the source provides a counter effect to the dose decreasing with increase diameter. In a larger vessel, the source can move a larger

distance closer to the vessel, which, as explained by the 1/r dose fall-off, leads to a greater dose amplification. This is the case for a source which is moving with a high frequency relative to the treatment time, which is a good assumption if one is considering motion imparted by the heart beating. One limitation is that the motion has been assumed to be random in all directions normal to the vessel axis, which may be too simple a model. It is easy to imagine the source spending more time on one side of the vessel and not being moved in both perpendicular axes to the same degree. In the absence of concrete data on the motion of the source, a random motion model was chosen to illustrate the possible size of the effect.

Tantalum was shown to have an outsized effect on vessel dosimetry compared to the other two metallic stents simulated. This is likely due to the much larger atomic number of tantalum than the metal alloys ($Z = 73$ compared to $Z_{eff} < 30$ for both stainless steel and nitinol). While tantalum is ductile and biocompatible [11], stents of the material should be avoided for implant in patients which will undergo IVBT because of its greater absorption of β-rays than other, lower Z materials. At 15% MSA and 0.1 mm thickness, tantalum was found to decrease dose to the vessel by over 10%, whereas nitinol and stainless steel each had less than a 5% effect. While this is by no means an exhaustive list of metals used in coronary stents, it is reasonable to assume that metals with similar atomic numbers will have similar effects on the vessel dosimetry. Advances in stent technologies will likely lead to thinner stents with lower MSA, decreasing the overall effect of the stents on vessel dose.

These findings of stent effect on vessel dose agree well with previous Monte Carlo studies of IVBT. Li [12] simulated stents of various materials and geometries in the presence of three different IVBT sources, including Sr-90/Y-90. For tantalum, nitinol, and stainless steel stents of 0.1 mm thickness and 20% MSA, he found stent factors ranging from 0.87 - 0.91, 0.94 - 0.98, and 0.93 - 0.98, respectively. Our simulations showed average stent factors for the entire vessel of 0.88, 0.97, and 0.94 under the same conditions, showing very close agreement. Li further simulated of stainless steel stents of varying MSA and found factors of 0.96, 0.94, and 0.92 for 10%, 20%, and 33% MSA, respectively. Our stainless steel simulations found 0.98, 0.94, and 0.91 stent factors for 10%, 20%, and 35% MSA, again showing agreement within 2%.

The dosimetric effect of the stent is also complicated by the fact that many patients undergo repeat interventions and stent placements. Lussier *et al.* [13] investigated using intra-vascular ultra sound (IVUS) to determine the number of stents present in section of coronary artery being treated. This image-based IVBT might be the only reliable method for determining the number of stents, since collecting patient angiograms and interventional records over possibly decades is not practical. They also use IVUS to give an estimate of the MSA, which they call stent density, of existing stents. Stents are categorized by the interpreter as either "low" (25%), "medium" (50%), or "high" (75%) densities. This is a subjective reading,

however, and MSA estimations may vary by interpreter.

Plaque has very limited ability to be visualized on fluoroscopy during angiogram, and plaque thickness would need to be measured with a separate imaging modality such as intravascular ultrasound to make use of the results of this study. The dosimetric effect of plaque was modeled under the assumption of a uniform thickness of plaque inside the vessel, which may not always be the case. Areas of the vessel with no plaque would not see any dose lost from absorption by the plaque and would only see minor diameter changes in the vicinity of plaque. Non-uniform plaques would lead to non-uniform doses in the vessel, where dose to each area of the vessel could be approximated by the thickness of the plaque covering that area. Areas with steep changes in plaque thickness are beyond the scope of this study as they would not be handled by the uniform thickness assumption and would need dedicated Monte Carlo studies.

5. Conclusion

This study allows for more accurate estimation of wall dose for Sr-90/Y-90 IVBT to coronary arteries. While it alone is not enough to conclude whether prescriptions should be updated in certain situations, further studies of patient outcomes post-IVBT could utilize this more accurate dosimetry to make definitive statements regarding the current prescriptions' efficacies. IVBT is generally less precise than other methods of radiation therapy, mostly owing to its small and variable targets, but accounting for the largest errors could bring it closer in line with the rest of radiation medicine practice.

Author Contribution Statement

Nicholas Coupera performed the Monte Carlo simulations, collected and analyzed the data, and prepared the initial draft of the manuscript. Jenghwa Chang served as the primary advisor for this project and had extensive discussions with Nicholas regarding the design and execution of the simulations. Drawing on his extensive clinical experience with IVBT, Yijan Cao provided valuable guidance on modeling clinical implementation.

Acknowledgements

The authors thank the Department of Radiation Medicine at Northwell for supporting this research.

Conflicts of Interest

The authors declare no conflicts of interest regarding the publication of this paper.

References

[1] Shlofmitz, E., Iantorno, M. and Waksman, R. (2019) Restenosis of Drug-Eluting Stents: A New Classification System Based on Disease Mechanism to Guide Treatment and State-of-the-Art Review. *Circulation*: *Cardiovascular Interventions*, **12**,

e007023. https://doi.org/10.1161/circinterventions.118.007023

[2] National Center for Health Statistics (NCHS) (2010) Number of All-Listed Procedures for Discharges from Short-Stay Hospitals, by Procedure Category and Age: United States, 2010. Centers for Disease Control and Prevention. https://urldefense.com/v3/__https://archive.cdc.gov/www_cdc_gov/nchs/data/nhds/4procedures/2010pro4_numberproceduregeage.pdf__;!!BWcElQ!wpGcGwf2lzh8miqU3Q0hx84Ve3AP-V9OyaNsJtrZdmVMEWa0Uju5DPElqOM-fGv4cUG5fPe4Zc3l9RIOLDYcbr7w$"https://archive.cdc.gov/www_cdc_gov/nchs/data/nhds/4procedures/2010pro4_numberproceduregeage.pdf

[3] Detloff, L.R., Ho, E.C., Ellis, S.G., Ciezki, J.P., Cherian, S. and Smile, T.D. (2022) Coronary Intravascular Brachytherapy for In-Stent Restenosis: A Review of the Contemporary Literature. *Brachytherapy*, **21**, 692-702. https://doi.org/10.1016/j.brachy.2022.05.004

[4] Nath, R., Amols, H., Coffey, C., Duggan, D., Jani, S., Li, Z., *et al.* (1999) Intravascular Brachytherapy Physics: Report of the AAPM Radiation Therapy Committee Task Group No. 60. *Medical Physics*, **26**, 119-152. https://doi.org/10.1118/1.598496

[5] U.S. Nuclear Regulatory Commission (2023) User's Manual: Beta-Cath 3.5F System. https://www.nrc.gov/docs/ML1410/ML14106A083.pdf

[6] Popma, J.J., Suntharalingam, M., Lansky, A.J., Heuser, R.R., Speiser, B., Teirstein, P.S., *et al.* (2002) Randomized Trial of ^{90}Sr/^{90}Y B-Radiation versus Placebo Control for Treatment of In-Stent Restenosis. *Circulation*, **106**, 1090-1096. https://doi.org/10.1161/01.cir.0000027814.96651.72

[7] Sarrut, D., Arbor, N., Baudier, T., Borys, D., Etxebeste, A., Fuchs, H., *et al.* (2022) The Opengate Ecosystem for Monte Carlo Simulation in Medical Physics. *Physics in Medicine & Biology*, **67**, Article 184001. https://doi.org/10.1088/1361-6560/ac8c83

[8] Chang, X., Huang, L., Liu, J., Cao, Y. and Chang, J. (2023) Monte Carlo Dosimetry of a Novel Yttrium-90 Disc Source for Episcleral Brachytherapy. *Journal of Applied Clinical Medical Physics*, **24**, e14140. https://doi.org/10.1002/acm2.14140

[9] Rahdert, D.A., Sweet, W.L., Tio, F.O., Janicki, C. and Duggan, D.M. (1999) Measurement of Density and Calcium in Human Atherosclerotic Plaque and Implications for Arterial Brachytherapy. *Cardiovascular Radiation Medicine*, **1**, 358-367. https://doi.org/10.1016/s1522-1865(00)00030-5

[10] Moselewski, F., O'Donnell, C.J., Achenbach, S., Ferencik, M., Massaro, J., Nguyen, A., *et al.* (2005) Calcium Concentration of Individual Coronary Calcified Plaques as Measured by Multidetector Row Computed Tomography. *Circulation*, **111**, 3236-3241. https://doi.org/10.1161/circulationaha.104.489781

[11] Chemicool (2025) Tantalum. Chemicool Periodic Table. https://www.chemicool.com/elements/tantalum.html

[12] Li, X.A. (2003) Dose Effects of Stents in Intravascular Brachytherapy for In-Stent Restenosis: A Monte Carlo Calculation. *International Journal of Radiation Oncology, Biology, Physics*, **55**, 842-848. https://doi.org/10.1016/s0360-3016(02)04280-3

[13] Lussier, L., Wallner, K., Kearney, K.E., Tiwana, J., Kim, E.Y., Parvathaneni, U., *et al.* (2023) Image-Guided Intravascular Brachytherapy Dose Escalation. *Brachytherapy*, **22**, 518-523. https://doi.org/10.1016/j.brachy.2023.04.004